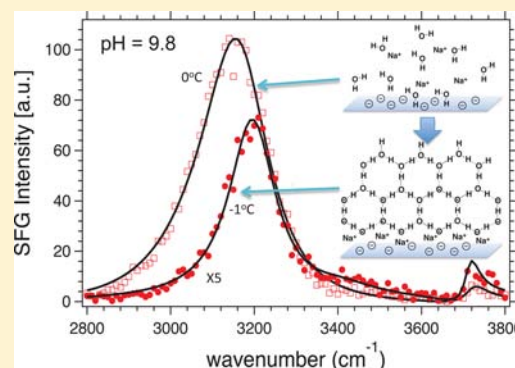# Freezing of Water Next to Solid Surfaces Probed by Infrared−Visible Sum Frequency Generation Spectroscopy

Emmanuel Anim-Danso,[†] Yu Zhang,[†] Azar Alizadeh,[‡] and Ali Dhinojwala*,[†]

[†]Department of Polymer Science, The University of Akron, Akron, Ohio 44325-3909, United States
[‡]GE Global Research, Niskayuna, New York 12309, United States

ABSTRACT: Ice formation next to solid surfaces is important in many biological, materials, and geological phenomena and may be a factor in how they impact various technologies. We have used sum frequency generation (SFG) spectroscopy to study the structure of ice as well as the freezing and melting transition temperatures of water in contact with sapphire substrates. We have observed that the structure of ice and water are a function of pH and the surface charge of the sapphire substrate. At low pH, we observed an increase in the SFG signal subsequent to ice formation. Contrary to expectations, at pH 9.8, corresponding to a negatively charged surface, the intensity of the ice SFG signal is about 10 times lower than that of water. Recent simulation studies have suggested that charge transfer is important for the high intensity of the ice peak at the ice−air interface. We believe that the segregation of sodium ions next to the negatively charged sapphire substrate may be responsible for disrupting the charge transfer and stitching bilayer at high pH, providing a plausible explanation for the experimental observations. Even though the structure of water and ice are affected by pH, the freezing and melting transition temperatures are independent of the surface charge. This report offers a unique insight on how ions next to solid surfaces could influence the structure of ice.

INTRODUCTION

Ice formation at solid interfaces is responsible for interstellar transport, cloud formation, catalysis of reactions for ozone destruction, and generation of lighting storms.[1−4] The state of water or ice layers next to solid surfaces is also of geological consequences in understanding friction between glaciers and is correlated with climate and life on earth. Questions regarding the freezing and melting of water next to solid surfaces have technological consequences in preventing ice formation and adhesion to surfaces of wind turbines and high-altitude aircrafts. Recently it was shown that freezing of water can be enhanced or delayed on positively or negatively charged surfaces, respectively.[5] Although this phenomena is of wide importance in many fields, there have been few experiments on the freezing of the first few layers of water molecules next to solid surfaces. Previous work on the freezing of ice next to silica surface has been performed by Wei et al.[6,7] In those experiments water was first frozen and then brought in contact with the silica surface. The authors found no premelting layer present at the interface. However, this geometry could not be used to study freezing of water in direct contact with the solid surface. In this work, we have extended the use of infrared−visible sum frequency generation (SFG) spectroscopy in conjunction with a unique sample cell to study the freezing of water next to Al_2O_3 (sapphire) surface as a function of pH.

SFG is a powerful surface-sensitive spectroscopic tool for studying water interfaces. In the dipole approximation, SFG, which is a second-order nonlinear technique, is only active where there is a breakdown in inversion symmetry. This selection rule makes it possible to use SFG to study the structure of molecules near surfaces and interfaces. Excellent reviews on this technique have been discussed elsewhere.[8−12] In brief, two incident beams, one visible (ω_{vis}) and the other a tunable IR beam (ω_{IR}), are temporally and spatially overlapped on the sample. Because of the non-zero second-order effects, a small fraction of the incident light is converted to sum frequency signal ($\omega_{SFG} = \omega_{vis} + \omega_{IR}$) at the interface. The SFG signals are enhanced when the tunable IR frequency overlaps with Raman and IR vibrational bands of molecules at the interface, making it possible to use this technique to identify the interfacial chemical groups. The intensity of the SFG signal, as a function of polarization of the incident and outgoing light carries information on the orientation of the interfacial molecules. For these reasons, SFG is an important tool to study orientation of interfacial water molecules, the hydrogen-bonding of interfacial water next to solid surfaces, and phase transition temperatures next to solid surfaces. SFG has been used to study water−solid[13−19] and ice−vapor surfaces.[6,7,20−23]

Sapphire surfaces in aqueous solutions have been the focus of study by several research groups because of their importance in both natural and industrial environments.[13,14,16−18,24,25] The sapphire surface OH groups can be de-protonated at high pH and protonated at low pH and the increase in SFG intensity

due to surface charges have been used to measure the isoelectric point (IEP) of the sapphire substrate.[13,14,18] Here, we have used sapphire prisms with isoelectric points between pH 5 and 6 as solid substrates. We have used pH variations as a means to change surface charges and to further study water–ice transition temperatures using SFG spectroscopy. A unique sample cell under vacuum allowed us to monitor the freezing and melting transitions *in situ* during both cooling and heating cycles between −50 and 25 °C. This work offers a unique insight on how ions can potentially influence the structure of ice formation next to charged surfaces, which in turn is crucial in understanding friction and adhesion of ice.

■ EXPERIMENTAL SECTION

The sapphire prisms were sonicated for 1 h in acetone, methanol, and deionized water. This was followed by sonication for 30 min in 10−15 mM HNO_3 and then rinsing thoroughly with deionized water. This cleaning method has been used to remove surface organic residues in previous studies and has been shown to give consistent results.[13,17,24,26] The stainless steel components of the sample cell were also cleaned by the same method. The sapphire prisms and the water cell were blow-dried using dry nitrogen gas followed by heating in an oven at 120 °C. In the past, we had observed small variations in the IEP among different sapphire prisms.[14] Therefore, for consistency, the data reported in this work were collected using the same prism. We have nonetheless verified that the specific conclusions are not affected by using different sapphire prisms. Ultrapure water from a Millipore filtration system (deionizing and organic removal columns) with a resistance of 18.2 MΩ/cm was used in these experiments. The pH of the water was adjusted using NaOH (≥97.0% pellets, Sigma-Aldrich) or HCl (37 wt%, Sigma-Aldrich) and the pH was measured using an Oakton pH meter with an epoxy-body pH electrodes.

Water condensation is a major issue when cooling the SFG sample cell below 0 °C, and thus, we designed a sample cell with a vacuum chamber as shown in Figure 1. The inside chamber containing the
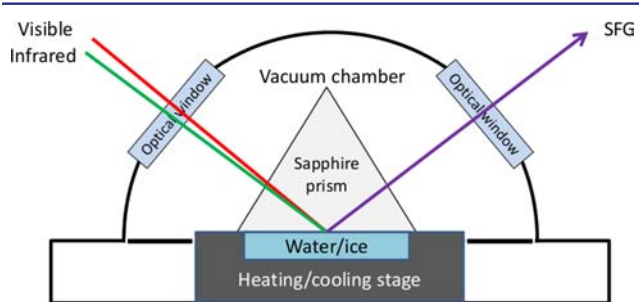

Figure 1. Diagram of the temperature stage and the sample geometry for SFG measurements. The water is sealed from one side by a sapphire prism, while the other side is in contact with a heating or cooling stage purchased from Instec Inc. The top part of the temperature cell was machined to hold CaF_2 and SiO_2 optical windows for the input and the output of the laser beams. The cell was held under vacuum to prevent water condensation on the sapphire prisms and to maintain a uniform temperature.

water was sealed to prevent any loss of water due to the vacuum. The temperature stage was purchased from Instec Inc. and modified in-house to hold the sapphire prisms. A steel dome was designed with CaF_2 window to introduce the visible and IR beams and SiO_2 window to collect the output SFG beam. The sample cell was designed with the flexibility to change the orientation of the windows to maintain the normal incidence of the input and output beams. A vacuum pressure of 8 Torr was used to prevent water condensation and to maintain temperature uniformity inside the sample chamber. The data in Figures 2−4 were collected with temperature increment of 1 °C (using

a 4 °C/min cooling and heating rate) and a 30 min equilibration time, before collecting the SFG spectra.

The SFG experiments were conducted using a picosecond Spectra Physics laser system with a tunable IR beam, 2000−3800 cm^{−1}, 1 ps pulse width, 1 kHz repetition rate, and a diameter of 100−200 μm, and a visible beam of 800 nm wavelength, 1 ps pulse width, 1 kHz repetition rate, and a diameter of 1 mm. These two beams were overlapped spatially and temporally on the sample. SFG signal is significantly enhanced when the IR overlaps with the resonant frequencies of the molecule being studied. A motorized, computer-controlled delay stage was used to ensure that the temporal delay was maintained while scanning IR frequencies from 2700 to 3800 cm^{−1}. The experiments were performed using sapphire prisms in total internal reflection geometry. This geometry provides an additional enhancement in the SFG signal if the incident beams are close to the critical angle.[27] A photomultiplier tube connected to a 0.5 m spectrometer in length was used to collect the SFG signals. All water spectra were collected at an IR incidence of 16° with respect to the face of the sapphire prism (60° angle prism). The incident angle of the visible laser beam was ~1.5° lower than the incident angles for the tunable IR laser. The polarization combinations reported in this work are SSP (s-polarized SFG output, s-polarized visible input, and p-polarized IR input) and PPP (p-polarized SFG output, p-polarized visible input and p-polarized IR input). The SSP and PPP polarizations probe different components of the molecular susceptibility tensor and are useful in interpreting the orientation of molecules. A model to interpret SSP polarization results in internal reflection geometry has been provided in previous publication.[28] We have used a Lorentzian fitting function to fit our data.[13]

$$I_{SFG} \propto \left| \chi_{eff,NR} + \sum \frac{A_q}{\omega_{IR} - \omega_q - i\Gamma_q} \right|^2 \tag{1}$$

In eq 1, $\chi_{eff,NR}$ describes the nonresonant contribution. A_q, Γ_q, and ω_q are the amplitude, damping constant, and angular frequency of the qth vibrational resonance, respectively.

■ RESULTS AND DISCUSSIONS

Figure 2 shows the SFG spectra in SSP polarization during cooling (a, c, and e) and heating cycles (b, d, and f) for pH values of 3.3 (a, b), 5.7 (c, d), and 9.8 (e, f). Figure 3 shows the SFG spectra in PPP polarization during cooling (a, c) and heating cycles (b, d) for pH values of 3.3 (a, b) and 5.7 (c, d). Figures 2 and 3 show two selected SFG spectra before and after freezing (melting) transitions from a series of spectra collected for different temperatures (for each of the pH values). The water and ice peaks are expected in the range of 3000−3800 cm^{−1}; typically, methyl and methylene assignments are in the range of 2700−3000 cm^{−1}. The absence of methyl and methylene hydrocarbon peaks validates the effectiveness of the cleaning process used for removing organic residues from the prism and sample cells. The spectral assignments for water have been discussed in previous publications.[12,15,18,19,29] The peaks at 3200 and 3450 cm^{−1} in the liquid spectra (a, c, and e) are assigned to strongly tetrahedrally coordinated (ice-like) and lower coordination (liquid-like) hydrogen-bond stretch, respectively.[12,18,19,29] These peaks are referred to as "ice-like" and "liquid-like" because they resemble the dominant peaks in IR and Raman spectra of ice and bulk water, respectively.[15,19] However, alternate assignments for the ice-like peak near 3200 cm^{−1} have been discussed recently in the literature.[30−34]

We have observed that above and below the IEP, the SFG intensity of the 3200 cm^{−1} ice-like peak is much greater than the 3450 cm^{−1} liquid-like water peak. The amplitude (A_q) for the 3200 cm^{−1} peak obtained after fitting the data using a Lorenztian equation (solid lines in Figure 2) is more than two
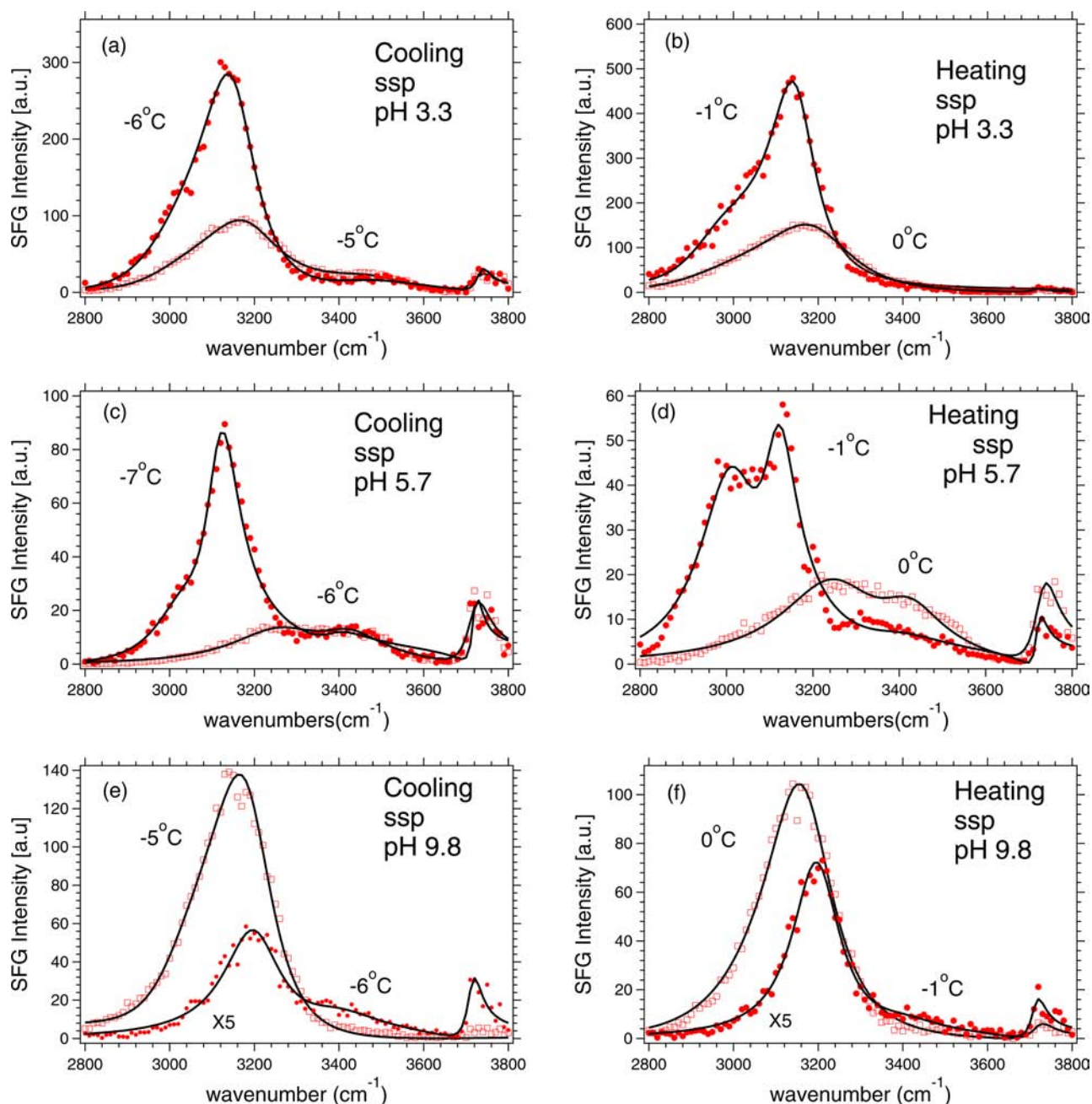
Figure 2. SFG spectra collected in SSP polarization during cooling (a, c, and e) and heating (b, d, and f) cycles. The data were collected with temperature increment of 1 °C (using a 4 °C/min cooling and heating rate), with a 30 min equilibration time before collecting the SFG spectra. The changes in the SFG spectra were measured for pH 3.3 (a,b), 5.7 (c,d), and 9.8 (e,f). The spectra for water (open squares) and ice (filled circles) near the freezing and melting transition temperatures are shown. The freezing transitions temperatures for the three pH conditions were between −5 and −6 °C, and the melting transition temperature was 0 °C.

times greater than the amplitude of the liquid-like peak at 3450 cm^{-1}. This is consistent with the explanation that the local electric field due to surface charges induces stronger hydrogen-bonding that resembles the tetrahedral bonding in ice.[13,18,35] For example, negative charges can cause a reorientation of the water molecules, with the oxygen atom facing the bulk and the hydrogen molecules pointing toward the surface.[13] This orientation seems to cause most of the water molecules in the interfacial region to hydrogen-bond to their neighboring molecules in an ordered and tetrahedral structure.[15] Near the IEP (Figure 2c,d), the 3200 and 3450 cm^{-1} peaks of the water

spectra are similar in strength and consistent with the concept of equal number of positive and negative surface charges.

In the liquid spectra (Figures 2a−d and 3a−d), the peak at ~3700 cm^{-1} has been assigned to surface hydroxyl groups on the sapphire surface.[13,25,36] Hass et al.[37] have shown that the sapphire surfaces have on average 10 OH groups per nm^2. These surface OH groups can be de-protonated at high pH (Figure 2e,f) and this observation has been used to measure the isoelectric point (IEP) of the sapphire substrate.[13,14,18] However, it is puzzling why the 3700 cm^{-1} peak in the water spectra (pH 3.3 and 5.7) is not shifted after contact with water. There have been two different explanations for the origin of the
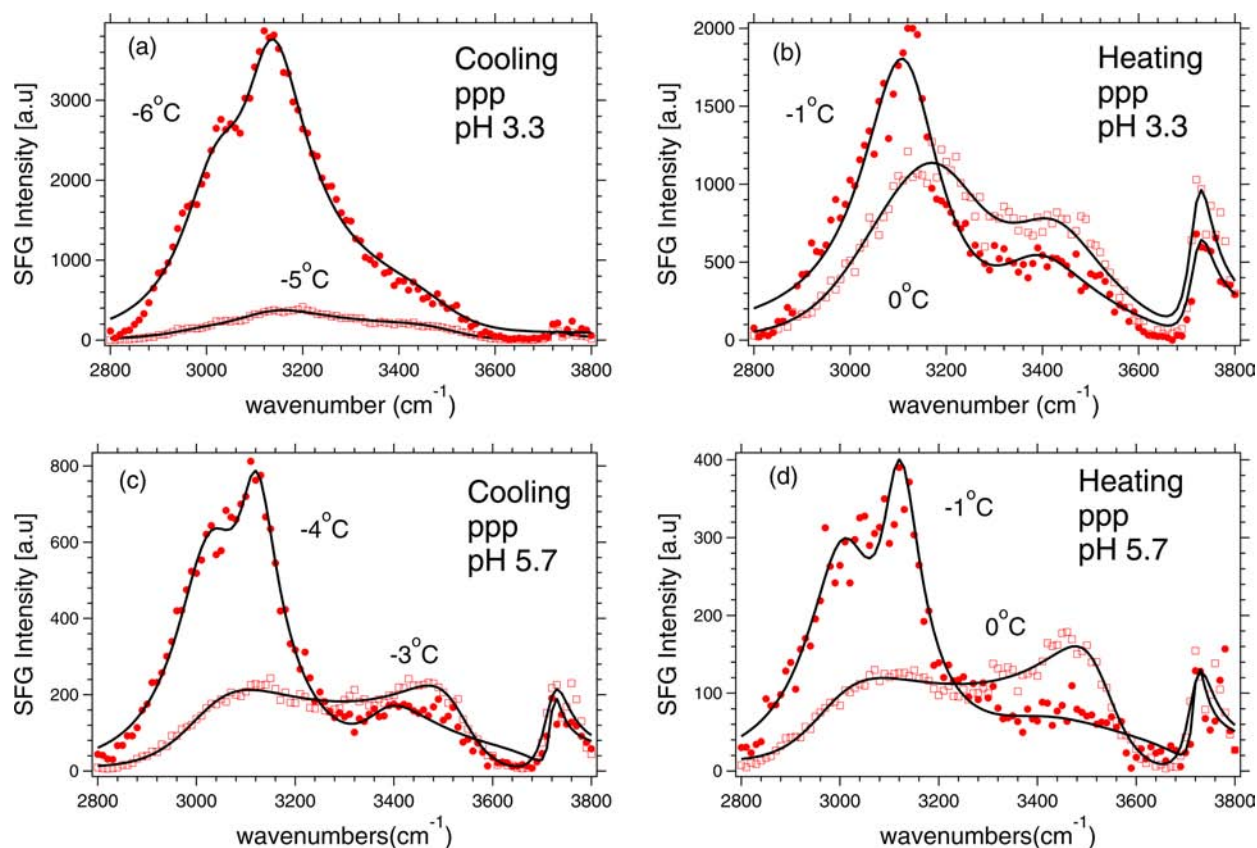
Figure 3. SFG spectra collected in PPP polarization during cooling (a,c) and heating (b,d) cycles. The data were collected using the conditions described in Figure 2. The changes in the SFG spectra were measured for pH 3.3 (a,b) and 5.7 (c,d). The open squares and filled circles correspond to temperatures where water or ice are in contact with the sapphire substrate, respectively. The freezing transitions temperatures for the three pH conditions were between −4 and −5 °C, and the melting transition temperature was 0 °C.

OH peak at the (0001) crystal plane. One study concluded that the $(Al)_nOH$ species are accessible to water, but do not form hydrogen bonds with water molecules.[13] Another study concluded that most of the OH groups may be in nanopores and do not interact with water and these OH groups are only accessible after annealing these surfaces at high temperature.[17] Our results indicate that the surface hydroxyl groups on the sapphire prisms are in contact with water (at pH 3.3 and 5.7) and they are de-protonated at conditions above the IEP.

In the ice spectra (Figures 2 and 3), the peak at ∼3150−3180 cm^{-1} is assigned to hydrogen-bonded stretching modes of the water molecules.[7] However, the origin of high intensity SFG ice peak is not obvious. The SFG experiments and theoretical models by Buch et al.[21] and Shultz et al.[22,23] for ice−vapor interface have suggested that the strong ice peak is due to water molecules that have one non-hydrogen-bonded free OH exposed to the vapor interface and the other OH that is part of a strong tetrahedrally coordinated hydrogen-bonded network. They also attributed the intense peak to the water molecules connecting the different bilayers (also called stitching bilayer). Groenzin et al.[22] used this model to explain experimental data from the basal ice face. This assignment was also supported by Barnett et al.,[23] using the polarization angle null SFG technique. Recently, Ishiyama et al. used molecular dynamics simulations to explain the high intensity of the ice peak at the ice−air interface.[38] They emphasized that the charge transfer between the bilayer stitching molecules and the bonded water molecules below is very important in explaining the intense ice peak in the SFG spectra for ice−air

interface. Because there is no direct theoretical work on ice−solid interface, we think that the high intensity of the SFG peak observed for ice−sapphire interface could be also related to the combination of charge transfer and stitching bilayer concept introduced for explaining the results for the ice−air interface.

Based on the assignments for the ice and water peaks in the SFG spectra, we will discuss the differences in the structure of water and ice as a function of pH. For pH 5.7, which is close to the IEP, the water spectra has strong ice-like and liquid-like peaks. At low and high pH, the ice-like peak is dominant in the water spectra. For pH 3.3 and 5.7, a strong ice peak was observed upon freezing (Figures 2a,c and 3a,c). A shoulder peak can be seen at ∼3000 cm^{-1} (more visible in the heating scans in Figures 2b,d and cooling and heating scans in Figure 3a,c,d), associated with stronger hydrogen-bonding of the water molecules at the sapphire−ice interface.[15]

In contrast, for pH 9.8, the ice-like peak in the water spectra blue-shifts (3180 cm^{-1}) upon freezing and is an order of magnitude weaker in intensity (Figure 2e,f). To understand the reasons behind this anomalous decrease in SFG intensity upon freezing we show a series of SFG spectra using SSP polarization in the cooling cycle as a function of temperature (Figure 4). As we cool further toward −50 °C, the peak red-shifts (which is the normal assignment for ice peak) and the SFG intensity increases but sill remains about 2 times lower than the water signal. During our experiments, we also observed that the SFG intensity increased rapidly upon freezing. However, in seconds, the SFG intensity sharply dropped again. Because of the rapid changes in the SFG intensity, we were unable to scan the IR
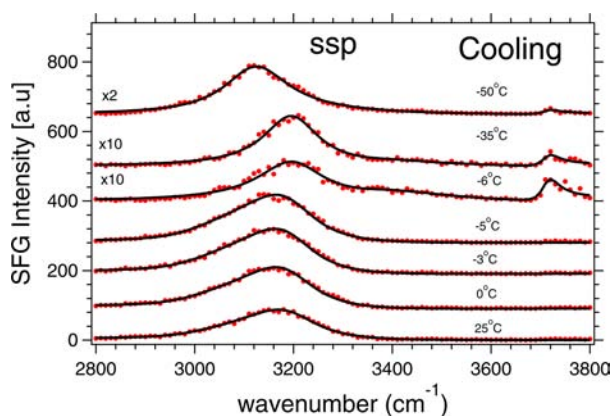
Figure 4. Complete set of SFG spectra collected in SSP polarization for pH 9.8 using the conditions described in Figure 2. Upon freezing, the dominate peak at 3150 cm^{-1} is shifted to 3210 cm^{-1}. In addition, there is a drop in intensity by a factor of 10 upon freezing. Between −35 and −50 °C, the SFG intensity increases, and the peak shifts back to 3150 cm^{-1}.

frequency to capture the complete spectra in such a short time. To overcome this challenge, we kept the IR frequency constant at 3180 cm^{-1} and monitored the changes in the SFG intensity during the cooling and heating cycles (rate of 4 °C/min) (Figure 5). We observed a sudden sharp increase in signal intensity that lasted for 10−20 seconds before decreasing below that of the liquid water signal (Figure 5a). It also shows a slight increase in signal as the ice is further cooled to −50 °C. This process was reversible upon heating (Figure 5b): there was first a drop in intensity as we heated from −50 °C toward the melting temperature, and then we observed a sharp increase in the SFG signal before the ice melted to liquid water.

This unusual change in the SFG intensity may be due to several factors and reflects the complexity of the transition of ice next to solid surfaces. Theoretical work on ice−air interface have shown that the SFG intensity of ice is not necessarily due to increase or decrease in orientational order.[38] As emphasized by Buch et al.[21] and Morita et al.,[38] charge transfer and the stitching bilayer are important in explaining the intensity of the ice peak. It is likely that for pH 9.8, the charge transfer and the stitching bilayer are perturbed at high pH, and this leads to decrease in the SFG intensity.

The hypothesis for the disruption of the charge transfer and stitching bilayer is the presence of sodium ions at the negatively charged sapphire interfaces. Based on the electrostatic interactions, we anticipate that sodium ions will be present in the vicinity of negatively charged sapphire substrate. In addition, the sodium ions could segregate at the sapphire interface during freezing of water. Past theoretical work by Pirzadeh and Kusalik[39] has shown that molecular solutes such as methane can induce defects at the ice−water interface. Carignana et al.[40,41] have performed molecular dynamics simulation studies of ice growth from supercooled NaCl ionic solution in the presence of free surfaces. They observed that ions were rejected to the surface from the bulk as the water froze. A study by Wei et al.[7] has shown that trace amount of ammonia in the aqueous solution had a dramatic influence as part of a 3-fold increase in the SFG signal intensity of the ice peak upon freezing next to the silica surface. They stipulated that ammonia molecules bind to the silanol groups, with two protons pointing into the bulk. This leads to increased ordering of the water molecules in the first layer and increased SFG signal upon freezing. Therefore, the hypothesis that sodium ions even at such low concentrations (63 μM) disrupt the ice structure (or the charge transfer) at the sapphire interface is plausible. For the case of pH 5.7, the surface is neutral and there is no preference for any segregation of ions. In the case of pH 3.3, the surfaces are positively charged with Cl$^-$ as a counterion. Thus we anticipate the Cl$^-$ ions to segregate to the sapphire surface. Furthermore, observation of the significant signal increase at the freezing transition suggests that Cl$^-$ ions are not as effective as Na$^+$ ions in perturbing the ice structure.

Finally, we would like to comment on the freezing and melting transition temperatures next to the sapphire surfaces as a function of pH. Ehre et al. showed that positive and negative charges enhanced and delayed freezing, respectively, at a LiTaO$_3$ surface.[5] The freezing transition temperatures for water in our study at pH 3.3, 5.7, and 9.8 are −6 ± 1, −5.5 ± 2, and −5.5 ± 0.7 °C, respectively (Figures 2 and 3). Because the freezing temperatures are dependent on nucleation, we have also measured the melting temperatures for all the three solutions during the heating cycles (Figures 2, 3, and 5). During the heating cycles, we observed a melting transition at 0 °C, similar to the bulk melting temperature of water. It is surprising that despite different structure of the water and ice layer for all
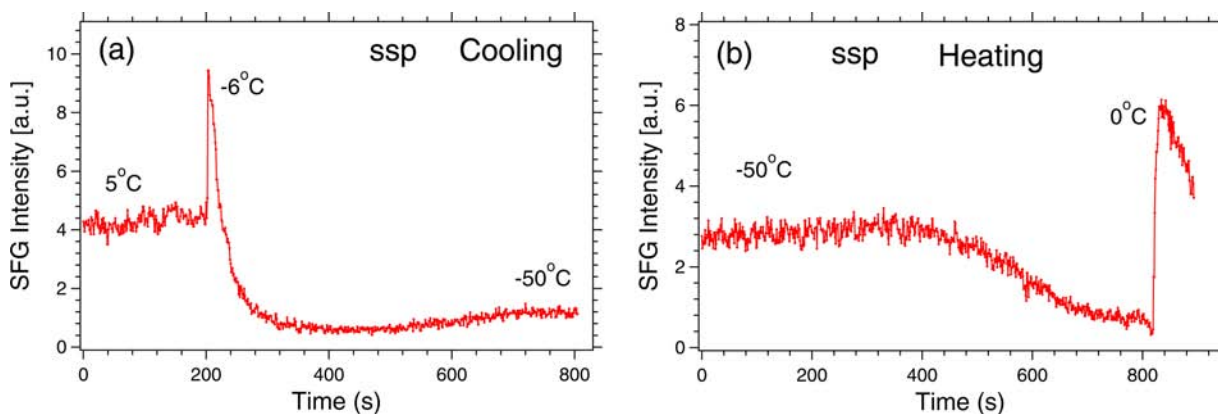

Figure 5. Variation in SFG intensity at pH 9.8 using SSP polarization and IR frequency of 3180 cm^{-1} during the cooling (a) and heating (b) cycles. These measurements were done at cooling and heating rates of approximately 4 °C/min. Freezing (−6 °C) and melting (0 °C) temperatures are labeled in the graphs.

three pH solutions, the melting and freezing transition temperatures in all cases are very similar.

The observation for pH 9.8 is particularly interesting because the SFG intensity decreased dramatically after freezing; we expected that if Na^+ ions were disrupting the ice-like structure, the freezing and melting temperature would have been different in comparison to bulk transition temperatures. We believe the transient change in SFG intensity is different from surface freezing observed for alcohol,[42] alkanes,[43] and polymers with alkyl side chains.[44] In the case of surface freezing for alkanes and alcohols, the surface crystalline layer was a thermodynamic stable state and the observation of this state did not depend on time. In Figure 4, when we provided enough time for equilibration we did not observe a clear two-step transition (one for the surface and the other for the bulk). The transient state observed in Figure 5 is perhaps due to sequence of events taking place near the surface during the ice formation and ice melting. If there is a difference in the two transition temperatures, it has to be small that we were unable to detect in these experiments. What is interesting is the second gradual transition at lower temperature beside the main freezing transition at -6 °C (and melting at 0 °C). We have also observed that the ice peak red-shifts between -35 and -50 °C, indicating a two-step transition for high pH. The first transition maybe related to formation of ice and also separation of Na^+ ions next to the sapphire surface. The Na^+-rich brine solution may freeze at a lower temperature (between -35 and -50 °C). This two-step transition may have important implications for use of these negatively charged surfaces in delaying ice formation.[5]

CONCLUSIONS

In summary, we have used SFG to study freezing and melting transition temperatures at sapphire–water interfaces for aqueous NaOH or HCl solutions at three different pH values of 3.3, 5.7, and 9.8. We observed different water spectra for each of the three pH solutions in both liquid and ice states. However, these differences had no effect on the freezing and melting transition temperatures. For pH 3.3 and 5.7 solutions, we observed a sharp increase in signal intensity upon freezing. In contrast, a two-step transition, with a significant reduction in the signal intensity at the transition temperature, was observed for pH 9.8. Based on recent theoretical studies on ice–vapor interfaces, we believe that the presence of Na^+ ions in the solution disrupts the charge transfer and the stitching bilayer, resulting in a drop in signal intensity. The SFG results presented here offer novel insight on how ions next to solid surfaces affect the structure of ice. Understanding the structure of ice next to solid surfaces is of importance in many areas of physical sciences, and our work clearly identifies the need for more direct theoretical models to fully understand the effect of ions on hydrogen-bonding network in ice and water.

AUTHOR INFORMATION

Corresponding Author
ali4@uakron.edu

Notes
The authors declare no competing financial interest.

ACKNOWLEDGMENTS

REFERENCES

(1) Heymsfield, A. J.; Miloshevich, L. M. *J. Atmos. Sci.* **1993**, *50*, 2335−2353.

(2) Molina, M. J.; Tso, T. L.; Molina, L. T.; Wang, F. C. *Science* **1987**, *238*, 1253−1257.

(3) Zuberi, B.; Bertram, A. K.; Koop, T.; Molina, L. T.; Molina, M. J. *J. Phys. Chem. A* **2001**, *105*, 6458−6464.

(4) Petrenko, V. F.; Whitworth, R. W. *Physics of Ice*; Oxford University Press: Oxford, U.K., 1999.

(5) Ehre, D.; Lavert, E.; Lahav, M.; Lubomirsky, I. *Science* **2010**, *327*, 672−675.

(6) Wei, X.; Shen, Y. R. *Appl. Phys. B: Lasers Opt.* **2002**, *74*, 617−620.

(7) Wei, X.; Miranda, P. B.; Zhang, C.; Shen, Y. R. *Phys. Rev. B* **2002**, *66*, 085401.

(8) Shen, Y. R. *The Principles of Nonlinear Optics*; Wiley: New York, 1984.

(9) Shen, Y. R. *Nature (London)* **1989**, *337*, 519.

(10) Eisenthal, K. B. *Chem. Rev.* **1996**, *96*, 1343−1360.

(11) Boyd, R. W. *Nonlinear Optics*, 3rd ed.; Academic Press: New York, 2008.

(12) Richmond, G. L. *Chem. Rev.* **2002**, *102*, 2693−2724.

(13) Zhang, L.; Tian, C.; Waychunas, G. A.; Shen, Y. R. *J. Am. Chem. Soc.* **2008**, *130*, 7686−7694.

(14) Hsu, P. Y.; Dhinojwala, A. *Langmuir* **2012**, *28*, 2567−2573.

(15) Ostroverkhov, V.; Waychunas, G. A.; Shen, Y. R. *Chem. Phys. Lett.* **2004**, *386*, 144−148.

(16) Nanjundiah, K.; Hsu, P. Y.; Dhinojwala, A. *J. Chem. Phys.* **2009**, *130*, 024702.

(17) Braunschweig, B.; Eissner, S.; Daum, W. *J. Phys. Chem. C* **2008**, *112*, 1751−1754.

(18) Yeganeh, M. S.; Dougal, S. M.; Pink, H. S. *Phys. Rev. Lett.* **1999**, *83*, 1179−1182.

(19) Ye, S.; Ma, S.; Wei, F.; Li, H. *Analyst* **2012**, *137*, 4981−4987.

(20) Wei, X.; Miranda, P. B.; Shen, Y. R. *Phys. Rev. Lett.* **2001**, *86*, 1554−1557.

(21) Buch, V.; Tarbuck, T.; Richmond, G. L.; Groenzin, H.; Li, I.; Shultz, M. J. *J. Chem. Phys.* **2007**, *127*, 204710.

(22) Groenzin, H.; Li, I.; Buch, V.; Shultz, M. J. *J. Chem. Phys.* **2007**, *127*, 214502.

(23) Barnett, I. L.; Groenzin, H.; Shultz, M. J. *J. Phys. Chem. A* **2011**, *115*, 6039−6045.

(24) Lützenkirchen, J.; Zimmermann, R.; Preočanin, T.; Filby, A.; Kupcik, T.; Küttner, D.; Abdelmonem, A.; Schild, D.; Rabung, T.; Plaschke, M.; Brandenstein, F.; Werner, C.; Geckeis, H. *Adv. Colloid Interface Sci.* **2010**, *157*, 61−74.

(25) Sung, J.; Shen, Y. R.; Waychunas, G. A. *J. Phys.: Condens. Matter* **2012**, *24*, 124101.

(26) Rabung, T.; Schild, D.; Geckeis, H.; Klenze, R.; Fanghänel, T. *J. Phys. Chem. B* **2004**, *108*, 17160−17165.

(27) Gautam, K. S.; Schwab, A. D.; Dhinojwala, A.; Zhang, D.; Dougal, S. M.; Yeganeh, M. S. *Phys. Rev. Lett.* **2000**, *85*, 3854−3857.

(28) Li, G.; Dhinojwala, A.; Yeganeh, M. S. *J. Phys. Chem. B* **2009**, *113*, 2739−2747.

(29) Shen, Y. R.; Ostroverchov, V. *Chem. Rev.* **2006**, *94*, 1140.

(30) Sovago, M.; Campen, R. K.; Wurpel, G. W. H.; Müller, M.; Bakker, H. J.; Bonn, M. *Phys. Rev. Lett.* **2008**, *100*, 173901.

(31) Walker, D. S.; Hore, D. K.; Richmond, G. L. *J. Phys. Chem. B* **2006**, *110*, 20451−20459.

(32) Gan, W.; Wu, D.; Zhang, Z.; Feng, R.; Wang, H. *J. Chem. Phys.* **2006**, *124*, 114705.

(33) Nihonyanagi, S.; Yamaguchi, S.; Tahara, T. *J. Am. Chem. Soc.* **2010**, *132*, 6867−6869.

(34) Skinner, J. L.; Pieniazek, P. A.; Gruenbaum, S. M. *Acc. Chem. Res.* **2012**, *45*, 93−100.

(35) Watanabe, M.; Brodsky, A. M.; Reinhardt, W. P. *J. Phys. Chem.* **1991**, *95*, 4593−4596.

(36) Liu, D.; Ma, G.; Allen, H. C. *Environ. Sci. Technol.* **2005**, *39*, 2025−2032.

(37) Hass, K. C.; Schneider, W. F.; Curioni, A.; Andreoni, W. *Science* **1998**, *282*, 265−268.

(38) Ishiyama, T.; Takahashi, H.; Morita, A. *J. Phys. Chem. Lett.* **2012**, *3*, 3001−3006.

(39) Pirzadeh, P.; Kusalik, P. G. *J. Am. Chem. Soc.* **2011**, *133*, 704−707.

(40) Carignano, M. A.; Shepson, P. B.; Szleifer, I. *Chem. Phys. Lett.* **2007**, *436*, 99−103.

(41) Carignano, M.; Baskaran, E.; Shepson, P.; Szleifer, I. *Ann. Glaciol.* **2006**, *44*, 113−117.

(42) Berge, B.; Konovalov, O.; Lajzerowicz, J.; Renault, A.; Rieu, J. P.; Vallade, M.; Als-Nielsen, J.; Grübel, G.; Legrand, J. F. *Phys. Rev. Lett.* **1994**, *73*, 1652−1655.

(43) Wu, X. Z.; Ocko, B. M.; Sirota, E. B.; Sinha, S. K.; Deutsch, M.; Cao, B. H.; Kim, M. W. *Science* **1993**, *261*, 1018−1021.

(44) Gautam, K. S.; Dhinojwala, A. *Phys. Rev. Lett.* **2002**, *88*, 145501.